

## A systematic study of suprathermal ions in TJ-II plasmas heated by electron cyclotron waves

B. Zurro<sup>1</sup>, A. Baciero<sup>1</sup>, D. Jiménez-Rey<sup>2</sup>, C. Clark<sup>3</sup> and A. Cappa<sup>1</sup>

<sup>1</sup>*Laboratorio Nacional de Fusión, Asociación Euratom-CIEMAT, Madrid, Spain*

<sup>2</sup>*Centro de Micro-Análisis de Materiales (CMAM), Universidad Autónoma de Madrid, Spain*

<sup>3</sup>*HSX Plasma Lab, University of Wisconsin, Madison, USA.*

**INTRODUCTION.** Previous works [1-3] carried out in the TJ-II stellarator have presented a technique for measuring the thermal ion temperature and information about suprathermal ion population using high resolution Doppler spectroscopy and an ion detector based on a luminescent probe. The present work studies the ion temperatures of the suprathermal component in hydrogen and helium discharges with spatial and time resolution. We compare, for selected discharges, the information on suprathermal confined ions provided by plasma spectroscopy with that of the luminescent probe on escaping ones.

The paper is organized as follows: first, a description of the spectral system is given along with a summary of the fluorescent probe; second, the plasma model used to justify the underpinnings of this work is presented; and finally, illustrative results obtained in TJ-II plasmas are given.

**EXPERIMENTAL SETUP AND DATA ANALYSIS.** The spectral line shapes of bulk ions have been recorded in TJ-II plasmas using two high spectral resolution spectrometers that view the plasma perpendicular to the main magnetic field through fiber guides. One of the spectrometers achieves spatial resolution by simultaneously sampling nine equally spaced lines of sight, which are shown in Fig. 1 of [3]. The channels are distributed so as to cover most of the plasma cross-section. The other spectrometer has better time resolution, but can only view one of the nine spatial channels at a time. The experimental systems and data analysis methods are described in more detail in [1] and [3].

The  $H_\alpha$  emission recorded by the spectrometers along each line-of-sight is fit to a superposition of three Gaussians, as explained and justified in [1]. We associate the narrowest Gaussian with the cold neutrals from the periphery and take the next broadest Gaussian to the thermal component because of its close relationship with the temperature measured by NPA. In this work, we focus on the behaviour of the temperature and magnitude of the broadest Gaussian, which we take to come from the suprathermal proton population. When the spectral system is measuring  $He^+$  line emission instead of  $H_\alpha$  emission, only two Gaussians are used

for the fit and the broadest one is again associated to the suprathermal component for these ions.

The luminescent probe has been operated for this experiment as a single channel system. The light produced by the ions impinging on the phosphor screen is collected and guided inside vacuum by a coherent fiber bundle to the vacuum break window. Just past this window is a filtered photomultiplier, which detects the total emission. The actual aperture, with the pinhole oriented at  $-32^\circ$  with respect to the local magnetic field, allows particles with pitch angles from approximately  $20^\circ$  to  $80^\circ$ , cogoing, to be detected.

**TYPICAL RESULTS.** There has been a large amount of research regarding the non-maxwellian electron energy distribution caused by ECRH [4, 5], and the non-maxwellian ion energy distribution caused by ICRH [6]. However, little research has been done, theoretically or experimentally, into the ion energy distribution in plasmas heated by second harmonic electron cyclotron waves. In part, this is probably because well-refined diagnostics suitable for such a study are scarce. Consequently, we cannot compare our results with similar findings from other similar fusion machines, nor we can be guided by theoretical predictions. Therefore, due to the novelty of even empirical observations on this subject, we will present a set of results on the behaviour of this suprathermal component of the majority species in TJ-II H<sub>2</sub> and in He plasmas and we will compare the time evolution of the energy content on the suprathermal component with measurements of the fast ion losses taken by a luminescent probe at the plasma edge.

In Figs. 1 (a) and (c) we present the temperature and the magnitude of the suprathermal tail along plasma chords numbered nine (top) to one (bottom), for a set of hydrogen discharges where the chord-average density was varied from 0.22 to  $1.05 \times 10^{19} \text{ m}^{-3}$ , and the injected ECRH power was varied from 200 to 510 kW. This set of data deserves a few comments: 1) The central chords (channel 5 and 6) show the largest change in tail temperature (400 to 800 eV) in response to changing plasma operational parameters; 2) The ions in TJ-II will grad-B drift towards the top of the machine at the measurement location, and the top channel measures a higher temperature than the bottom one; similar effect has been reported with the neutral particle analyzer (NPA) in TJ-II [7]; 3) The temperature profile of the ion tail exhibits a small variation across the plasma radius.

Figs. 1 (b) and 1 (d), show data taken from Helium discharges where the He<sup>+</sup> (4686 Å) emission line was fit to two Gaussians. The temperatures of the broadest Gaussians are plotted in Fig. 1 (c) as a function of the spatial channel number for a range of densities ( $0.44 - 1.06 \times 10^{19} \text{ m}^{-3}$ ) and injected powers (400 to 600 kW). All discharges correspond to on-axis

heating, except #20321, which was heated off-axis and with non-zero  $n_{\parallel}$  (parallel wave vector) and has the highest values of temperature (square black points). The chord-integrated emission intensity of the He ions is depicted, in Fig. 1 (d) for the same set of discharges.

In Fig. 2 we plot the time evolution of the suprathermal tail temperature and intensity for selected discharges in hydrogen and helium. In Fig. 2 (a) we show the temperature time evolution of the  $\text{He}^+$  suprathermal temperature and emission intensity for two discharges with the same density ( $0.4 \times 10^{19} \text{ m}^{-3}$ ), but with different injected on-axis power (190 and 265 kW). Notice that both the average temperature, as indicated by the straight lines, and the average emission intensity are higher for higher heating power. This behavior contrasts with that of the thermal component (not shown) for which there is no change in temperature. In Fig. 2 (b) we compare the evolution of the suprathermal tail in hydrogen and helium in otherwise similar discharges with a line-average density of  $0.4 \times 10^{19} \text{ m}^{-3}$ . Notice that the tail temperature of the  $\text{He}^+$  is higher than that of the protons in hydrogen discharges where both have been measured.

Finally, in Fig. 3, we compare the suprathermal component of confined protons, as measured by spectroscopy, with the behavior of the fast ions ( $E > 1 \text{ keV}$ ) that are lost from the plasma and are subsequently detected by the luminescent probe. The results are shown in Fig. 3, where we have plotted the time evolution of the relative energy content of the suprathermal tail, which was estimated by taking the product of the area of the corresponding Gaussian and the temperature, along with the total light detected by the luminescent probe (Fast Ion Detector Losses). Notice that, for the discharges, depicted in Fig. 3 (a), the time behaviors of both magnitudes are very similar. A similar comparison for almost flat, low density discharges ( $0.3 \times 10^{19} \text{ m}^{-3}$ ) is shown in Fig. 3 (b) where the discrepancy between the traces of FIDL and the time evolution of the suprathermal energy content in the plasma is obvious, being more dramatic for the discharge #24381 with an ECRH deposition radius of  $\rho = 0.63$ , than in #24382, where the deposition is at  $\rho = 0.33$ . We must emphasize that whereas the spectroscopic technique probes the energy content dominantly in the direction perpendicular to the main magnetic field, the luminescent ion probe senses mainly ions with pitch angles between  $20^\circ$  and  $80^\circ$ . Therefore, the strong discrepancy between both signatures might be an indication of decoupling between perpendicular and parallel ion behavior.

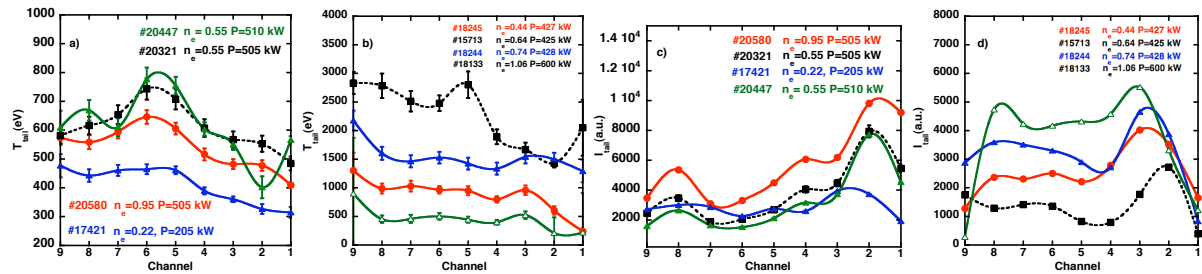


**Figure 1.** Spatial dependence of suprathermal tail temperatures and magnitudes for protons and  $\text{He}^+$  in  $\text{H}_2$  and He discharges, respectively: a) Temperature chord-integrated profiles for protons in hydrogen discharges under different conditions; b) Similar plot for He; c) Intensity profiles of the data displayed in (a) for protons; d) Similar plot for He. The electron density is given in the plot, in units of  $10^{19} \text{ m}^{-3}$ , along with the total injected power.

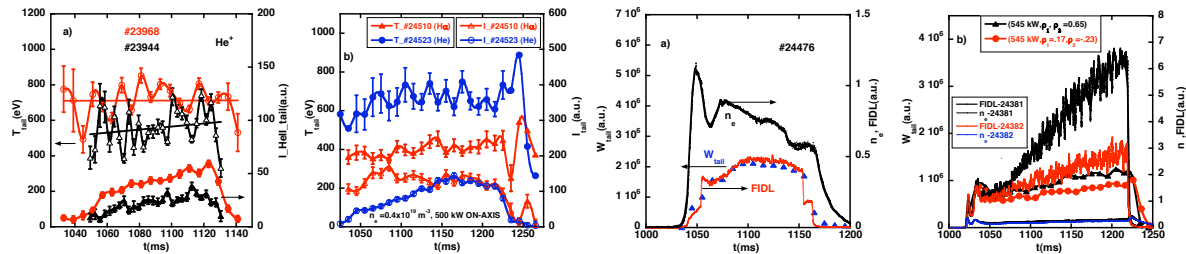


**Figure 2.** Temporal evolution of the suprathermal tail temperatures and intensities: a) For  $\text{He}^+$  in two He discharges with different ECRH injected powers; b) Comparison of tail temperature and intensity evolution for proton and helium in two discharges with hydrogen as filling gas.

**Figure 3.** Comparison of the luminescent probe (FIDL) signal with the relative energy content of the suprathermal tail measured by the spectroscopic method: a) For a moderate density discharge where both traces match well; b) Similar comparison for two low density discharges with different off-axis heating.

**ACKNOWLEDGEMENTS.** This work was partially funded by the Spanish Ministry of Science and Education under Project No. ENE2007-65007. D.J.R. acknowledges the *Juan de la Cierva* program of the MICINN, JCI-2009-05681, for financial support.

## References

- [1] D. Rapisarda, B. Zurro, V. Tribaldos et al., *Plasma Phys. Control. Fusion* **49**, 309 (2007).
- [2] D. Jiménez-Rey, B. Zurro, J. Guasp, et al., *Rev. Sci. Instrum.* **79**, 93511 (2008).
- [3] A. Baciero, B. Zurro B, K. J. McCarthy, *Rev. Sci. Instrum.* **72**, 971(2001).
- [4] A. I. Meshcheryakov et al., *Plasma Physics Reports* **32**, 103 (2006).
- [5] F. Medina et al., *Plasma Phys. and Control. Fusion* **49**, 385 (2007).
- [6] H. Okada et al., *Nuclear Fusion* **47**, 1346 (2007).
- [7] J. M. Fontdecaba, R. Balbín et al., Proc. 29<sup>th</sup> Conf. EPS Montreux, **26B**, P-5.030 (2002).